FEBS Letters 585 (2011) 1951–1956

FEBS Letters

journal homepage: www.FEBSLetters.org

Enzyme kinetic studies of histone demethylases KDM4C and KDM6A: Towards understanding selectivity of inhibitors targeting oncogenic histone demethylases

Jan B.L. Kristensen [a], Anders L. Nielsen [a,b], Lars Jørgensen [a], Line H. Kristensen [a], Charlotte Helgstrand [a], Lina Juknaite [a], Jesper L. Kristensen [a], Jette S. Kastrup [a], Rasmus P. Clausen [a], Lars Olsen [a], Michael Gajhede [a,*]

[a] Department of Medicinal Chemistry, Faculty of Pharmaceutical Sciences, University of Copenhagen, Universitetsparken 2, DK-2100 Copenhagen, Denmark
[b] Novo Nordisk A/S, Biopharm Chemistry, Novo Nordisk Park 1, DK-2760 Måløv, Denmark

ARTICLE INFO

Article history:
Received 11 March 2011
Accepted 4 May 2011
Available online 12 May 2011

Edited by Christian Griesinger

Keywords:
Histone lysine demethylases
Oncogenic
Tumor repressor
Enzyme kinetics
Ligand selectivity

ABSTRACT

To investigate ligand selectivity between the oncogenic KDM4C and tumor repressor protein KDM6A histone demethylases, KDM4C and KDM6A were enzymatically characterized, and subsequently, four compounds were tested for inhibitory effects. 2,4-dicarboxypyridine and (*R*)-*N*-oxalyl-*O*-benzyltyrosine (3) are both known to bind to a close KDM4C homolog and 3 binds in the part of the cavity that accommodates the side chain in position 11 of histone 3. The inhibition measurements showed significant selectivity between KDM4C and KDM6A. This demonstrates that despite very similar active site topologies, selectivity between Jumonji family histone demethylases can be obtained even with small molecule ligands.

1. Introduction

The organization of chromatin plays an important role in gene regulation. The state of chromatin is determined by covalent modifications of the DNA itself or of the histones that organizes DNA in the nucleosomes. One such modification is methylation of lysines in the *N*-terminal regions of in particular histones H3 and H4 [1]. These methylations were thought to be irreversible until the discovery of lysine specific demethylase LSD1 [2]. Shortly after, another family of histone lysine-specific demethylases (HDMs) was discovered [3]. These enzymes are dioxygenases containing a Jumonji C (JmjC) domain with an active site containing Fe(II) and the co-factor α-ketoglutaric acid.

In 2006, the discovery of the HDM KDM4C, a histone 3 lysine 9 (H3K9) demethylase was published. It was shown that inhibition of this HDM decreases tumor cell proliferation [4], and the gene had previously been found to be up regulated in cell lines derived from esophageal squamous carcinomas [5]. This suggested KDM4C to be an oncogene, thus making the development of inhibitors an important issue. A number of inhibitors against KDM4C and the closely related KDM4A and KDM4E have recently been disclosed [6–9], and the binding mode of a number of them have been established, since 3D structures are available of the catalytic cores (cc) of KDM4A [10], KDM4C (PDB code 2XML, unpublished) and KDM4D (PDB code 3DXT, unpublished).

In 2007, the histone 3 lysine 27 (H3K27) specific HDM denoted KDM6A was discovered, and shown to be important for the regulation of HOX genes that are central during cellular differentiation [11]. Results accumulated during the later years suggest that KDM6A acts as a tumor repressor [12–15]. Thus, in terms of the potential of JmjC HDM inhibitors as anti-cancer agents, it appears crucial that inhibitors targeting KDM4C do not affect KDM6A function and activity. The 3D structure of KDM6A is currently unknown, however, the structure of the cc of the closely related KDM6B has recently been deposited in PDB (PDB code 2XXZ, unpublished). This enables structural comparison as a tool to identify differences in the active site architecture and, through this comparison, to obtain inhibitors that display selectivity between KDM4C and KDM6A.

Using the oncogenic KDM4C and tumor repressor protein KDM6A as model system, we show that selective inhibition of KDM4C by small molecule inhibitors is achievable. Furthermore, we demonstrate that inhibition of KDM4C by targeting of the specific part of the active site accommodating position 11 of the histone 3 peptide substrate, based on a strategy described elsewhere

Abbreviations: cc, catalytic core; cc4C, catalytic core of KDM4C; cc6A, catalytic core of KDM6A; 2,4-DCP, 2,4-dicarboxypyridine; FDH, formaldehyde dehydrogenase; H3K9, histone 3 lysine 9; H3K27, histone 3 lysine 27; HDM, histone lysine-specific demethylase; IMAC, immobilized metal affinity chromatography; JmjC, Jumonji C; **1**, (*R*)-*N*-oxalyl-tyrosine; **2**, (*R*)-*O*-benzyltyrosine; **3**, (*R*)-*N*-oxalyl-*O*-benzyltyrosine; NOG, *N*-oxalylglycine; SEC, size exclusion chromatography

* Corresponding author. Fax: +45 35 33 60 41.
E-mail address: mig@farma.ku.dk (M. Gajhede).

0014-5793/$36.00 © 2011 Federation of European Biochemical Societies. Published by Elsevier B.V. All rights reserved.
doi:10.1016/j.febslet.2011.05.023

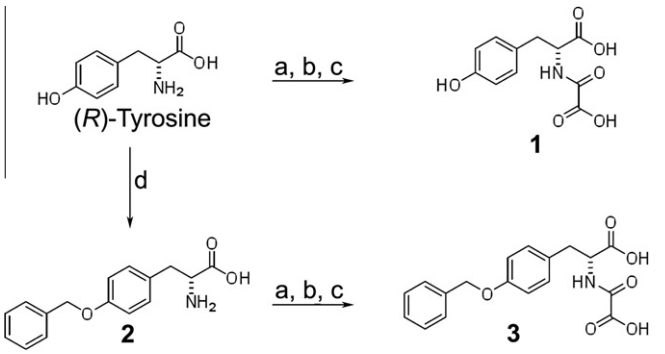

Fig. 1. Synthesis of compounds **1**–**3** from (*R*)-tyrosine. (a) $SOCl_2$, CH_3OH, reflux, 4 h; (b) monomethyl oxalylchloride, toluene, reflux, 4 h; (c) 1 M NaOH, r.t., 2 h, then ion-exchange; (d) $CuSO_4$, NaOH, benzylbromide, H_2O/CH_3OH, r.t., 16 h, and then neutralization.

[8], can lead to KDM4 subtype-selective inhibitors. Moreover, since the kinetic characterizations of these proteins have not been reported, we present the kinetic characterization of the catalytic cores of KDM4C (cc4C) and KDM6A (cc6A). Based on the kinetic characterizations, we identify H3 peptide substrates suitable for screening purposes and utilize these to identify KDM4C selective inhibitors.

2. Materials and methods

2.1. General

All chemicals used for buffers, co-factors, lysozyme, DNAse, formaldehyde dehydrogenase (FDH) from *Pseudomonas putida*, *N*-oxalylglycine (NOG), 2,4-dicarboxypyridine (2,4-DCP), α-cyano-4-hydroxy cinnamic acid and polystyrene NBS™ treated 384 wells plates used for FDH assay were from Sigma–Aldrich, Denmark. Solvents for MALDI-TOF were of HPLC-grade and from Merck, Denmark. EDTA free protease inhibitor cocktail tablets used in protein purification were from Roche. Histone tail H3K9me3 and H3K27me3 synthetic peptide substrates were purchased from Peptide 2.0, USA or generously donated by Novo Nordisk A/S, Denmark. The plasmid coding for cc4C (1–349) was generously donated by the Biotech Research and Innovation Center (BRIC), Denmark. The pOPIN vector F was generously donated by the Oxford Protein Production Facility, Great Britain. All reagents and solvents for the synthesis of (*R*)-*N*-oxalyl-tyrosine (**1**) and (*R*)-*N*-oxalyl-*O*-benzyltyrosine (**3**) were purchased from Sigma–Aldrich, Denmark or VWR, Denmark and used without further purification. NMR spectra were recorded on a 300 MHz Varian spectrometer at room temperature (r.t.). Elemental analysis was performed at the University of Vienna, Austria. Melting points were determined in an open capillary tube and are uncorrected.

2.2. Cloning, expression and purification of cc4C and cc6A

The detailed procedures are supplied in Supplementary information. In summary, the *N*-terminal His-tagged proteins were expressed in *Escherichia coli* using auto-induction [16] and purified by immobilized metal affinity chromatography (IMAC) and size exclusion chromatography (SEC).

2.3. Synthesis of compounds ***1***–***3***

Compounds **1** and **3** were both synthesized starting from (*R*)-tyrosine (Fig. 1). *O*-Benzylation of (*R*)-tyrosine to produce (*R*)-*O*-benzyltyrosine (**2**) was done similar to the procedure of Otake and Izawa [17]. The *N*-oxalyl amino acids, **1** and **3**, were produced

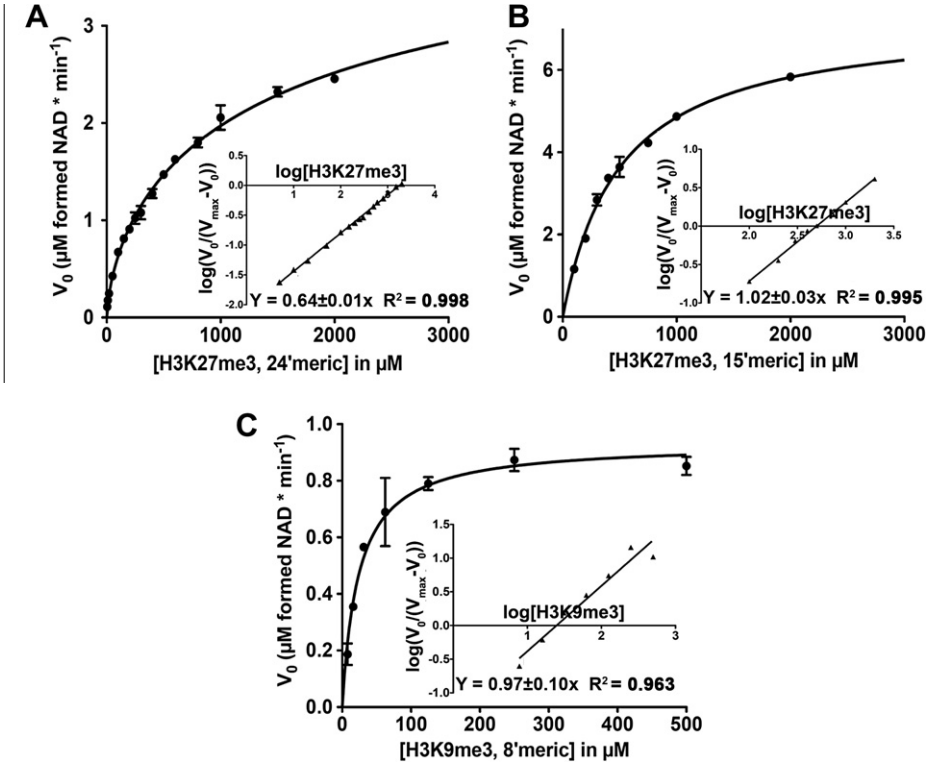

Fig. 2. Enzyme kinetic plots of 25 µM cc6A for synthetic 24- and 15-meric H3K27me3 substrates and 2.5 µM cc4C for 8-meric H3K9me3 substrate. Initial velocity (V_0) (µM formed NADH min^{-1}) as a function of concentration of peptide substrate in µM. (A) The kinetic profile of the 24-meric peptide substrate at cc6A. (B) The kinetic profile of the 15-meric peptide substrate at cc6A. (C) The kinetic profile of the 8-meric peptide substrate at cc4C. Corresponding Hill plots have been inserted to illustrate the negative cooperativity observed for the 24-meric HeK27me3 substrate. Error bars represent one standard deviation (S.D.).

using a method described elsewhere [18]. The detailed procedure is stated in Supplementary information.

2.4. Enzyme kinetics and inhibition studies

For determination of enzyme kinetics and inhibition studies of cc4C and cc6A, a FDH coupled assay was set up, essentially as described elsewhere [19]. Experiments were carried out in 384 wells, low volume, flat bottomed solid black NBS™ surface treated polystyrene plates (Corning) and on the same batch of protein. Assay buffer consisted of 50 mM HEPES, pH 7.5, 50 mM NaCl, 500 μM α-ketoglutaric acid, 0.5–5 mM ascorbate, 2 mM NAD^+, 0.05–0.5 U FDH and 50–500 μM Fe(II). Assays were carried out in triplicate measurements in 10% DMSO at 37 °C and the total reaction volume was 25 μl. For the determination of kinetics parameters, 2.5 μM cc4C was incubated with 8-meric H3(7–14)K9me3 peptide substrate ARK(me3)STGGK (7.8–500 μM) and 25 μM cc6A was incubated with 24-meric H3(21–44)K27me3 ATKAARK(me3)SAPATGGVKKPHRYRPG (5–2000 μM), 15-meric H3(20–34)K27me3 LATKAARK(me3)SAPATGG (5–2000 μM) and 9-meric H3(23–31)K27me3 KAARK(me3)SAPA (5–2000 μM) substrates. For inhibition studies, 5 μM cc4C and 12.5 μM cc6A were incubated for 30 min with various concentrations of ligands before adding 100 μM of H3K9me3 in the case of cc4C and 500 μM H3K27me3 in the case of cc6A. The formation of NADH, measured as an increase in relative fluorescence units, were monitored with a Safire2™ microplate reader (Tecan) in 30 s cycles over a period of minimum 15 min (up to 24 h) and converted to μM NADH formed min^{-1} using a NADH standard curve (Supplementary Fig. S1). Excitation wavelength and emission wavelength was 355 nm and 460 nm, respectively. For inhibition studies, the 8-meric cc4C (100 μM) and 15-meric cc6A (500 μM) substrates were used. Reaction mixtures of assay buffer without substrate were used as negative controls. For curve fitting and data analysis, GraphPad Prism® 5.0 was used.

2.5. MALDI-TOF

The enzymatic reaction was carried out as described and quenched by addition of 50% (v/v) of 1% TFA. The reaction mixture was diluted 1:9 with a saturated solution of α-cyano-4-hydroxycinnamic acid in 65% acetonitrile, in MilliQ water containing 0.1% TFA. One milliliter was spotted onto the target and air dried for 15 min at r.t. The MALDI-TOF MS was carried out on an Ultraflex TOF/TOF (Bruker) operated in positive ion mode with an ion source voltage of 25 kV, a lens voltage of 7.5 kV and a reflector voltage of 26.3 kV. The system was run in deflection mode with a mass suppression of 500 Da. The data analysis was carried out using the FlexAnalysis software (Bruker). Baseline subtraction and smoothing of the curves was applied.

2.6. GRID analysis

The GRID program version 22 [20] was used to characterize the binding pockets of cc4A and cc6B using the C3 probe.

3. Results and discussion

3.1. The ccs of KDM4C and KDM6A

Approximately 2 mg of purified cc4C (1–349) and cc6A (940–1401) was obtained pr. liter expression media. Initial protein purity after IMAC purifications were approximately 60–75%. The protein purity after SEC was higher than 90% as assessed by SDS–PAGE (Supplementary Fig. S2).

3.2. Enzyme kinetics of cc4C and cc6A

To identify histone 3 peptide substrates suitable for screening purposes, a series of H3K27me3 peptides were tested. The results show that different cc6A peptide substrates resulted in different kinetic profiles. The 24-meric H3K27me3 substrate exhibited a negative cooperative kinetic profile with a Hill slope of 0.64, while the 15-meric substrate exhibited Michaelis–Menten kinetics (Fig. 2). Turnover of a shorter (9-meric) peptide was not detected by FDH assay or by MALDI-TOF. Based on the kinetic studies, the 15-meric peptide substrate was chosen for inhibition studies. With regard to cc4C, only an 8-meric peptide was tested, since this substrate has frequently been used in cc4A, cc4C and cc4E inhibition studies [7,8]. This substrate also exhibited Michaelis–Menten kinetics (Fig. 2). Various concentrations of Fe(II) (50–500 μM) and FDH (0.05–0.5 U) did not alter the turnover of peptide substrates. The kinetic parameters K_{prime}/K_m, k_{cat} and k_{cat}/K_m of cc6A and cc4C for the various peptide substrates are summarized in Table 1. The difference in K_m/K_{prime} and K_{cat} indicates that the 15-meric substrate may have a lower binding affinity, but a higher turnover. However, comparison of the substrate specificity constants (k_{cat}/K_m values) reveals that cc6A demethylates the 24-meric substrate approximately 2.5-fold more efficiently than the 15-meric substrate. Also, the kinetics revealed that KDM4C is a more efficient enzyme than KDM6A, when comparing the substrate specificity constants. General enzymatic activity was confirmed by MALDI-TOF MS. The H3K27me3 cc6A substrates were primarily demethylated to H3K27me2, but in case of the 24-meric substrate also to trace amounts of the monomethylated species (Supplementary Fig. S3). This correlates with previous findings for full length KDM6A incubated with core histones [11,21]. An 8-meric H3K9me3 cc4C substrate was primarily demethylated to H3K9me2 but also to the monomethylated species (Supplementary Fig. S3). This observation is in agreement with previous findings for the full length protein, in which a 40-meric synthetic substrate and core histones were used [4].

Table 1
K_{prime}/K_m, k_{cat} and k_{cat}/K_m values of cc6A and cc4C for various H3K27me3 and H3K9me3 peptide substrates. In addition, IC_{50} values of four inhibitors are given. One S.D. is reported for each value. Note that for the 24-meric peptide substrate, a K_{prime} value is listed instead of a K_m value, due to negative cooperativity. N.D: Not detectable by FDH-coupled assay or MALDI-TOF MS.

Substrate	Enzyme	K_{prime}/K_m (μM)	k_{cat} (min^{-1})	k_{cat}/K_m (min^{-1} μM^{-1} × 10^3)
H3(21–44)K27me3 24-meric	cc6A	139.5 ± 15.1	0.19 ± 0.04	1.36 ± 0.29
H3(20–34)K27me3 15-meric	cc6A	495.4 ± 34.7	0.29 ± 0.01	0.58 ± 0.05
H3(23–31)K27me3 9-meric	cc6A	N.D	N.D	N.D
H3(7–14)K9me3 8-meric	cc4C	23.9 ± 3.9	0.37 ± 0.06	15.5 ± 3.5

Enzyme	Ligands	NOG	2,4-DCP	**1**	**3**
cc6A	IC_{50} (μM)	531 ± 14	177 ± 12	≫1000	≫625
cc4C	IC_{50} (μM)	681 ± 14	2.4 ± 0.1	281 ± 15	135 ± 16

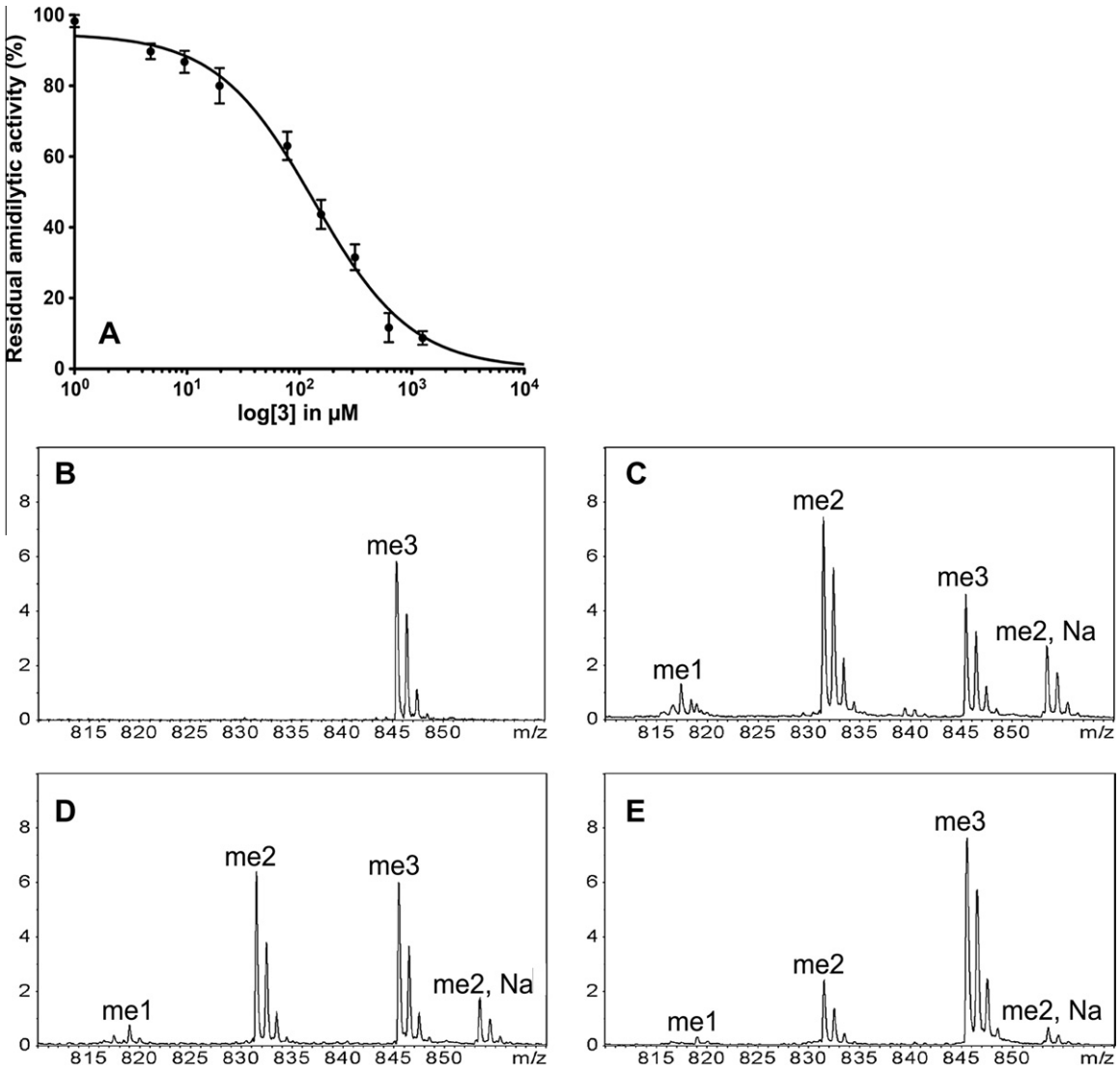

Fig. 3. Inhibition data of compound **3** at cc4C and representative MALDI-TOF MS spectra. (A) IC_{50} curve of **3**. (B–E) MALDI-TOF MS spectra of 100 μM 8-meric peptide incubated with: (B) reaction buffer (negative control); (C) 5 μM cc4C; (D) 5 μM cc4C and 78 μM **3**; (E) 5 μM cc4C and 1.25 mM **3**. All intensities are in relative units. The additional top at approximately 854 in (C–E) is a me2, Na adduct. Error bars represent one S.D.

3.3. Inhibition studies on cc4C and cc6A

For inhibition studies, the four compounds, NOG, 2,4-DCP, **1** and **3** were tested (Table 1). In the case of cc4C, all four tested ligands have inhibitory effect, in agreement with previous findings for cc4A, cc4C and cc4E [7–9]. NOG, the inactive amide analog of α-ketoglutaric acid, inhibited both cc4C and cc6A with comparable IC_{50} values, suggesting the same binding mode of NOG to cc4C and cc6A. In contrast, the IC_{50} of 2,4-DCP was almost a factor 75 higher for cc6A (177 μM) than for cc4C (2.4 μM), demonstrating subtype selectivity. This difference in affinity may be explained by structural comparison of the crystal structures of cc4A with 2,4-DCP bound [7] and cc6B (PDB code 2XXZ, unpublished), a close homolog to cc6A (84% sequence similarity of the cc region [21]). In cc4A (and cc4C), Lys241 interacts with the carboxylic group in position 2 of 2,4-DCP (Fig. 4C). In cc6A and cc6B, Lys241 corresponds to Asp1440. Furthermore, this residue is positioned away from the cc, due to differences in a backbone loop (Fig. 4C), causing a loss of interaction that most likely causes a significant decrease in affinity, as observed.

Compounds **1** and **3** inhibited cc4C in the μM range (281 and 135 μM, respectively). It has previously been shown that **3** is a KDM4 selective inhibitor, when compared to factor-inhibiting hypoxia-inducible factor, another JmjC containing dioxygenase [8,22]. Similarly, we observed no inhibition of cc6A at 625 μM, indicating selectivity of **3** towards KDM4C compared to KDM6A. For compound **3**, an IC_{50} curve and representative MALDI-TOF MS spectra for the inhibition of KDM4C are shown in Fig. 3. Comparison of the structures of cc4A (in complex with **3** (PDB code 2WWJ), NOG and an 8-meric H3K9me3 substrate (PDB code 2OQ6)) and cc6B (PDB code 2XXZ), shows that the amino acids surrounding **3** are different in cc4A (and cc4C) compared to cc6B (and cc6A). For example, in the crystal structure of cc4A (Fig. 4A), **3** makes favorable van der Waals interactions with the surrounding amino acids, with the benzyloxy phenyl group of **3** occupying position 11 of the substrate [8]. In the cc6B structure, **3** does not fit well into the pocket (Fig. 4B), when superimposing it to cc4A. Moreover, in cc4A, a weak hydrogen bond between the oxygen atom of **3** and the backbone amide nitrogen of Ala186 was reported [8]. This interaction is not possible in cc6B and presumably also not in cc6A, because Ala186 (cc4A) corresponds to Pro1385 (cc6B).

Taken together, we have shown that selective inhibition of cc4C, in the low μM range, by small molecule ligands is achievable.

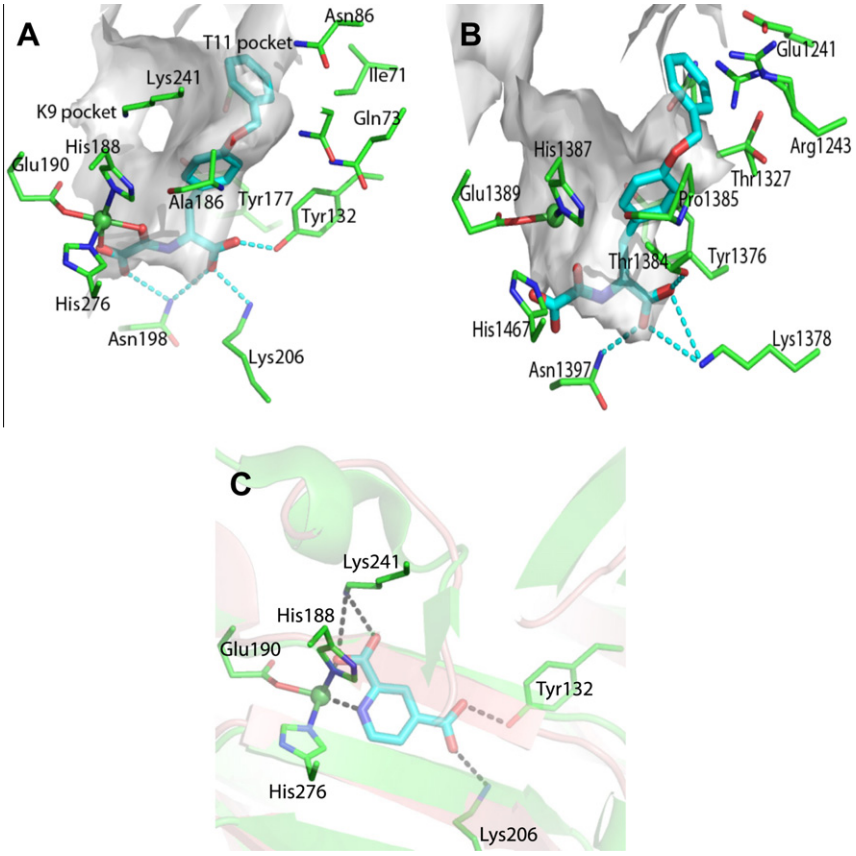

Fig. 4. Structural comparison of cc4A and cc6B. (A) Crystal structure of cc4A (PDB code 2WWJ [8]) in complex with **3** (cyan C atoms). (B) Crystal structure of cc6B (PDB code 2XXZ) superimposed with 2WWJ. (C) Ribbon representation of the crystal structure of cc4A in complex with 2,4-DCP (cyan C atoms) superimposed with 2XXZ. Gray surface shows isosurface at −0.1 kcal/mol of the C3 probe, indicating favorable vdW interactions.

However, optimization of the scaffolds is necessary for the development of new inhibitors exhibiting high affinity and selectivity towards the KDM4 HDM subtypes. Such inhibitors may provide a new strategy for future cancer treatment.

Acknowledgements

The authors wish to thank the Biotech Research and Innovation Center (BRIC) for the cc4C construct, Oxford Protein Production Facility for pOPIN vector F, and Novo Nordisk A/S for conducting MALDI-TOF MS experiments and donation of synthetic peptide substrates. The Lundbeck Foundation is acknowledged for financial support to J.B.L.K. The University of Copenhagen programme of excellence on epigenetics is acknowledged for financial support.

Appendix A. Supplementary data

Supplementary data associated with this article can be found, in the online version, at doi:10.1016/j.febslet.2011.05.023.

References

[1] Mosammaparast, N. and Shi, Y. (2010) Reversal of histone methylation: biochemical and molecular mechanisms of histone demethylases. Annu. Rev. Biochem. 79, 155–179.
[2] Shi, Y., Lan, F., Matson, C., Mulligan, P., Whetstine, J.R., Cole, P.A., Casero, R.A. and Shi, Y. (2004) Histone demethylation mediated by the nuclear amine oxidase homolog LSD1. Cell 119, 941–953.
[3] Tsukada, Y., Fang, J., Erdjument-bromage, H., Warren, M.E., Borchers, C.H., Tempst, P. and Zhang, Y. (2006) Histone demethylation by a family of JmjC domain-containing proteins. Nature 439, 811–816.
[4] Cloos, P.A.C., Christensen, J., Agger, K., Maiolica, A., Rappsilber, J., Antal, T., Hansen, K.H. and Helin, K. (2006) The putative oncogene GASC1 demethylates tri- and dimethylated lysine 9 on histone H3. Nature 442, 307–311.
[5] Yang, Z.Q. et al. (2000) Identification of a novel gene, GASC1, within an amplicon at 9p23-24 frequently detected in esophageal cancer cell lines. Cancer Res. 60, 4735–4739.
[6] King, O.N.F. et al. (2010) Quantitative high-throughput screening identifies 8-hydroxyquinolines as cell-active histone demethylase inhibitors. PLoS ONE 5, e15535.
[7] Rose, N.R. et al. (2008) Inhibitor scaffolds for 2-oxoglutarate-dependent histone lysine demethylases. J. Med. Chem. 51, 7053–7056.
[8] Rose, N.R. et al. (2010) Selective inhibitors of the JMJD2 histone demethylases: combined nondenaturing mass spectrometric screening and crystallographic approaches. J. Med. Chem. 53, 1810–1818.
[9] Hamada, S. et al. (2010) Design, synthesis, enzyme-inhibitory activity, and effect on human cancer cells of a novel series of jumonji domain-containing protein 2 histone demethylase inhibitors. J. Med. Chem. 53, 5629–5638.
[10] Chen, Z. et al. (2006) Structural insights into histone demethylation by JMJD2 family members. Cell 125, 691–702.
[11] Agger, K. et al. (2007) UTX and JMJD3 are histone H3K27 demethylases involved in HOX gene regulation and development. Nature 449, 731–734.
[12] Dalgliesh, G.L. et al. (2010) Systematic sequencing of renal carcinoma reveals inactivation of histone modifying genes. Nature 463, 360–363.
[13] Terashima, M., Ishimura, A., Yoshida, M., Suzuki, Y., Sugano, S. and Suzuki, T. (2010) The tumor suppressor Rb and its related Rbl2 genes are regulated by Utx histone demethylase. Biochem. Biophys. Res. Commun. 399, 238–244.
[14] Tsai, M.-C., Wang, J.K. and Chang, H.Y. (2010) Tumor suppression by the histone demethylase UTX. Cell Cycle (Georgetown, TX) 9, 2043–2044.
[15] van Haaften, G. et al. (2009) Somatic mutations of the histone H3K27 demethylase gene UTX in human cancer. Nat. Genet. 41, 521–523.
[16] Studier, F.W. (2005) Protein production by auto-induction in high density shaking cultures. Protein Expr. Purif. 41, 207–234.
[17] Otake, Y. and Izawa, K. (2005) Process for producing aminoepoxide. Patent US 2005/0137408 A1, Ajinomoto Co. Inc., Japan.
[18] Cunliffe, C.J., Franklin, T.J., Hales, N.J. and Hill, G.B. (1992) Novel inhibitors of prolyl 4-hydroxylase. 3. Inhibition by the substrate analogue *N*-oxaloglycine and its derivatives. J. Med. Chem. 35, 2652–2658.

[19] Couture, J.F., Collazo, E., Ortiz-Tello, P.A., Brunzelle, J.S. and Trievel, R.C. (2007) Specificity and mechanism of JMJD2A, a trimethyllysine-specific histone demethylase. Nat. Struct. Mol. Biol. 14, 689–695.
[20] Goodford, P.J. (1985) A computational procedure for determining energetically favorable binding sites on biologically important macromolecules. J. Med. Chem. 28, 849–857.
[21] Hong, S., Cho, Y.-W., Yu, L.-R., Yu, H., Veenstra, T.D. and Ge, K. (2007) Identification of JmjC domain-containing UTX and JMJD3 as histone H3 lysine 27 demethylases. Proc. Natl. Acad. Sci. USA 104, 18439–18444.
[22] Shi, Y. and Whetstine, J.R. (2007) Dynamic regulation of histone lysine methylation by demethylases. Mol. Cell 25, 1–14.